

PAPER • OPEN ACCESS

Pseudo-Hall Effect in Graphite on Paper Based Four Terminal Devices for Stress Sensing Applications

To cite this article: Afzaal Qamar *et al* 2017 *J. Phys.: Conf. Ser.* **829** 012004View the [article online](#) for updates and enhancements.

Related content

- [Stress measurement in a cantilevered silicon beam undergoing coupled motion of torsion and bending](#)
Markus Egretzberger, Andreas Kugi, Stefan Günthner *et al.*
- [Electrical Properties of \$Al/Al_2O_3/\(Ba,Rb\)BiO_3/SrTiO_3\(Nb\)\$ Three Terminal Device](#)
Fumihiko Toda, Tomoyuki Yamada, Katsufumi Hashimoto *et al.*
- [Dislocation Damping in Graphite Doped with IC1](#)
Michihiro Saito and Takuro Tsuzuku

Recent citations

- [Toan Dinh *et al*](#)

**IOP | ebooks™**

Bringing together innovative digital publishing with leading authors from the global scientific community.

Start exploring the collection—download the first chapter of every title for free.

Pseudo-Hall Effect in Graphite on Paper Based Four Terminal Devices for Stress Sensing Applications

Afzaal Qamar¹, Tuba Sarwar², Toan Dinh¹, A.R.M. Foisal¹, Hoang-Phuong Phan¹ and Dzung Viet Dao^{1,3}

¹ Queensland Micro-Nanotechnology Centre, Griffith University, Queensland, Australia

² DPAM, PIEAS, P. O. Nilore, Islamabad, Pakistan

³ School of Engineering, Griffith University, Queensland, Australia

Abstract. A cost effective and easy to fabricate stress sensor based on pseudo-Hall effect in Graphite on Paper (GOP) has been presented in this article. The four terminal devices were developed by pencil drawing with hand on to the paper substrate. The stress was applied to the paper containing four terminal devices with the input current applied at two terminals and the offset voltage observed at other two terminals called pseudo-Hall effect. The GOP stress sensor showed significant response to the applied stress which was smooth and linear. These results showed that the pseudo-Hall effect in GOP based four terminal devices can be used for cost effective, flexible and easy to make stress, strain or force sensors.

1. Introduction

In recent years, researchers have paid much attention to paper based devices for diagnostics, electronics and microfluidics applications [1-3]. Flexible and wearable electronics is the fundamental part of flexible appliances which require ultra-thin and flexible navigation modules, force sensing, body tracking, and relative position monitoring systems. Soft robotics and transient electronics are the ultimate beneficiaries of these flexible and wearable electronics. The main advantages of this technology are the low cost, diversity in material choice, disposability and ease of fabrication [4]. Graphite on paper (GOP), in which graphite layers are deposited on paper by either graphite-ink printing techniques [5-6], or manual pencil drawing techniques, has been utilized as the sensing element in flexible sensors for strain sensing and chemical analysis [7-12].

Most of the previous work on GOP based stress/strain sensors is based on the conventional two terminal resistor sensors which suffer several drawbacks. They show high temperature sensitivity relative to stress response. To increase the total resistance, resistors are often designed with large meandering patterns which suffer from transverse sensitivity [13]. On the other hand pseudo-Hall effect device inherently utilizing the high accuracy of four-wire resistance measurement method can overcome the limitations of the conventional resistor sensors which show less temperature sensitivity and can be made small enough to capture the localized stress [14]. It can also eliminate the use of Wheatstone bridge for stress measurement which is used in simple resistor based strain sensors. A large number of studies can be found on Si based pseudo-Hall devices and SiC based pseudo-Hall device [15-21] but according to our knowledge there has been no report on the pseudo Hall effect in Graphite on paper based devices. Therefore, in this study we report a GOP based cost effective and flexible stress/strain sensor based on pseudo-Hall effect.



2. Characterization of the Graphite on Paper

In order to investigate the properties of the Graphite drawn on paper, scanning electron microscopy and Raman spectroscopy were used. Figure 1(a) shows the SEM image of the paper substrate. It can be observed that the paper substrate consists of cellulose fibre and is porous which helps the graphite particles to imbed in it. Figure 1(b) shows the SEM image of the Graphite trace on paper. It can be observed from Fig. 1(b) that a continuous and uniform trace of Graphite was obtained. In order to analyse the carbon networks and defect density inside the pencil trace Raman spectroscopy was utilized. Figure 1(c) shows the Raman spectra of the GOP trace. There are three main peaks observed in the Raman spectra corresponding to three different bands D, G and 2D at wavenumbers of 1350 cm^{-1} , 1580 cm^{-1} and 2725 cm^{-1} , respectively. The D band corresponds to the number of defects and boundaries, while the G band indicates the number of sp^2 bonded carbon networks in the Graphite trace. As the Graphite trace is made by pencil drawing the presence of the defects and boundaries is obvious by this technique but the enough carbon networks are present inside the trace for the establishment of current flow. Additionally, the 2D band corresponds to the type of stacking sequence in a direction perpendicular to the graphite plane. Figure 1(d) shows the photograph of a four terminal device ($500 \mu\text{m} \times 500 \mu\text{m}$) made from pencil trace and after making the contacts by silver epoxy.

3. Fabrication of Devices

Figure 2 shows the fabrication process of the device. A simple pencil with 6B grade was used to draw Graphite trace on to a paper substrate (Fig. 2(a)). After the pencil trace low resistive aluminium tape and silver epoxy (186–3616, RSC components) were used to make the electrical contacts to the devices as shown in Fig. 2(b). The fabricated devices with silver epoxy contacts were then cured on a hotplate (Fig. 2(c)). The paper substrate was then cut into stripes to apply stress for pseudo Hall effect measurements (Fig. 2(d)). The Ohmic behaviour of the fabricated devices was analysed using HP 4145B analyser, indicating a good Ohmic contact between the electrodes and the graphite trace. The input current to the device was applied at terminals 1 and 2 while the output voltage was observed at terminals 3 and 4 as indicated in Fig. 1(d). The contacts for input current was made strip like in order to have the uniform effect of stress in the device while the output contacts were made point like to have the minimum deviation in the output signal. Four terminal devices with different geometries were made and analysed for pseudo-hall effect including, square shape, rectangular shape and Hall cross shape but the square shape is presented here as it produced the maximum output response to stress.

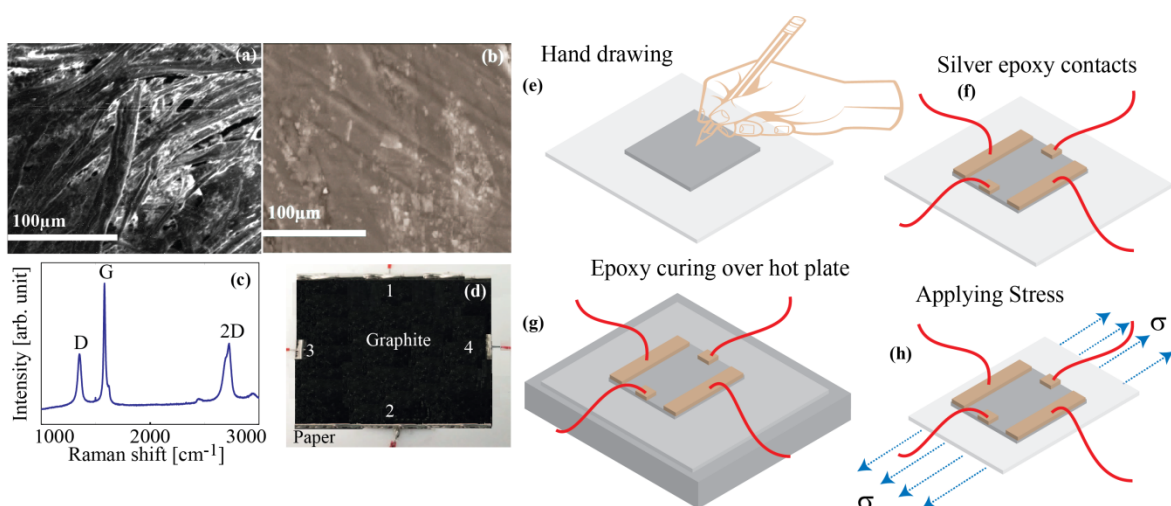


Figure 1: (a) SEM image of paper substrate, (b) SEM image of GOP drawn by pencil, (c) Raman spectra of GOP, (d) GOP four terminal device made from pencil drawing and contacts from silver epoxy, (e) schematic of the pencil drawing on paper, (f) fabrication of electrical contacts by silver epoxy, (g) curing of the epoxy to get stable Ohmic contacts, (h) cutting of the paper strip containing devices into strips to apply stress.

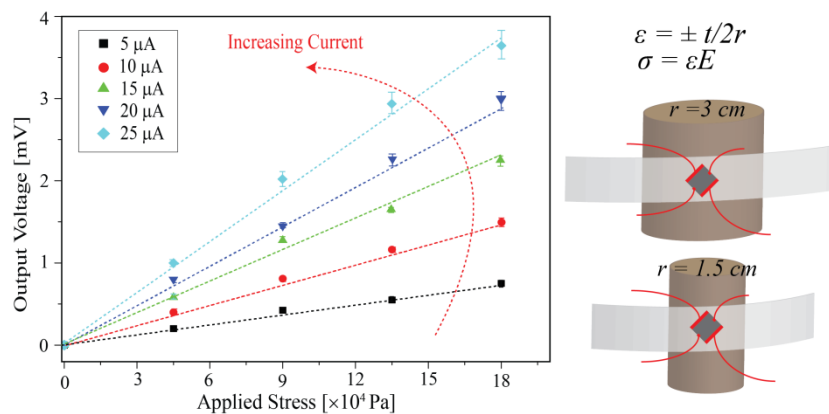


Figure 2: Pseudo-Hall effect in GOP square device. The output voltage of the device varies significantly as the stress is varied. The output voltage also increases linearly with increasing the value of input current. The stress was applied to the device by wooden cylinders having different diameters.

4. Results and discussion

The stress to the devices was applied by bending the paper substrate, containing graphite device, around wooden cylinders of different diameters. Different diameters of the cylinder produced different strain to the graphite devices according the relation; $\varepsilon = t/2r$. Here, t is thickness of the paper substrate, which is $90 \mu\text{m}$ and r is the radius of the wooden cylinder. The correspond stress induced to the devices was calculated by Hooke's law; $\sigma = \varepsilon E$, where E is the Young's modulus of the paper having a value of 0.03 GPa [22]. When stress is applied to the device at a constant input current at terminals 1 and 2, a variation in output voltage at terminals 3 and 4 can be observed, which is called pseudo-Hall effect. Figure 2(a) shows the variation of output voltage of the device against various levels of applied stress to the device. It can be observed that the output voltage of the device varies significantly when the applied stress to the device is varied and this variation is linear against the applied stress. This shows that the pseudo-Hall effect in GOP based devices can be used as a measure of stress/strain, force and pressure.

The output response of the device was observed at different angles within the plane of the paper. Figure 3 shows the variation of output voltage of the device against applied stress when the device is rotated within the plane of the paper. The square device was fabricated at different angles with respect to the plane of the paper. The output response of the device was different for different angles within the plane of the paper. The maximum output response was only observed when the direction of input current was at an angle of 45° with the direction of applied stress. The minimum out response was observed when the angle between direction of current and applied stress was 0° or 90° . Therefore, the output voltage against applied stress varies between maximum and minimum values as the device is rotated in the plane of paper.

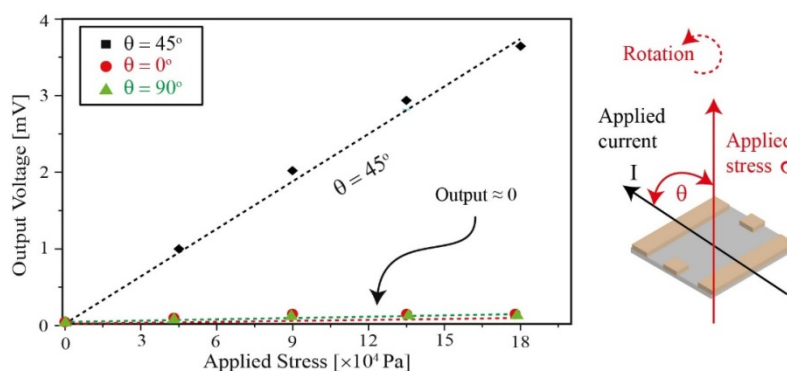


Figure 3: Output response of the device when device is rotated at different angles within the plane of the paper substrate.

In order to analyse the repeatability of the output response of the device against applied stress, the stress was applied to the device in steps. Figure 4 (a) shows the output response of the device when stress was applied and removed in steps of 10 sec. It can be observed that the response of the device to applied stress is repeatable and comes to initial value after each step when stress is removed. Figure 4(b) shows the variation of output voltage of the device against input current at a fixed value of the external applied stress. It can be observed from Fig. 4(b) that the output response of the device also increases linearly when the input current is increased. This feature of the device is very important as the output signal of the device can be raised to any measurable level by just increasing the input current to the device. This is not true in case of a simple piezoresistor in which a resistor produces change in resistance which is same at all input current values. The compressive stress/strain behaviour of these devices could not be observed due to the damage of the device when it is compressed, facing the wooden roller. This problem can be eliminated by laminating the paper after making the device and ohmic contacts.

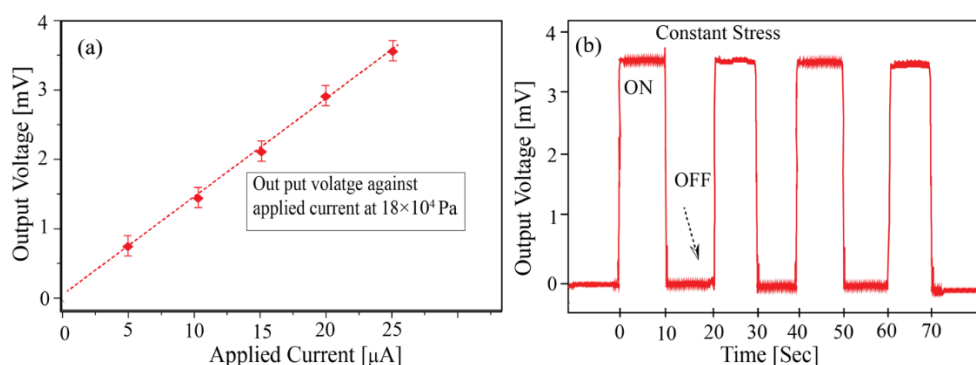


Figure 4: (a) Variation of output voltage with varying current and constant stress, (b) step response of the device showing repeatable behaviour.

Acknowledgments

This work was performed in part at the Queensland node of the Australian National Fabrication Facility, a company established under the National Collaborative Research Infrastructure Strategy to provide nano and micro-fabrication facilities for Australia's researchers. This work has been partially supported by the Griffith University's New Researcher Grants.

References

- [1]. Cai X, Peng M, Yu X, Fu Y and Zou D 2014 *J. Mater. Chem. C* **2**(7) 1184–1200.
- [2]. Nie Z, Deiss F, Lui X, Akbulut O and Whitesides G M 2010 *Lab Chip* **10** 3163–3169.
- [3]. Bracher P J, Gupta M and Whitesides G M 2010 *J. Mater. Chem.* **20** 5117–5122.
- [4]. Mahadeva S K, Walus K and Stoeber B 2015 *ACS Appl. Mater. Interfaces* **7** 8345–8362.
- [5]. Akter T, Joseph J and Kim W S 2012 *IEEE Electron Device Lett.* **33**(6) 902–904.
- [6]. Liu X, Mwangi M, Li X, O'Nrien M and Whitesides G M 2011 *Lab Chip* **11**(13) 2189–2196.
- [7]. Lin C W, Zhao Z, Kim J and Huang J 2014 *Sci. Rep.* **4** 3812.
- [8]. Liao X, Liao Q, Yan X, Liang Q, Si H, Li M and Zhang Y 2015 *Adv. Funct. Mater.* **25**(16) 2395–2401.
- [9]. Phan H P, Dao D V, Dinh T, Brooke H, Qamar A, Nguyen N T, Zhu Y 2015 *Proc. 28th IEEE Int. Conf. Micro Electro Mechanical Systems (MEMS)*, Estoril 825–828.
- [10]. Kang T K 2014 *Appl. Phys. Lett.* **104** 073117.
- [11]. Dinh T, Phan H P, Dao D V, Woodfield P, Qamar A, Nguyen N T 2015 *J. Mater. Chem. C* **3** 8776–8779

- [12]. Dinh T, Phan H P, Qamar A, Nguyen N T, Dao D V 2016 RSC Advances **6** (81) 77267-77274
- [13]. Mian A, Suhling J C and Jaeger R 2006 IEEE Sens. J. **6** 340–356
- [14]. Doelle M, Mager D, Ruther P and Paul O 2006 Sens. Actuators A **127** 261.
- [15]. Qamar A, Dao D V, Han J, Phan H P, Younis A, Tanner P, Dinh T, Wang L, Dimitrijević S 2015 Journal of Materials Chemistry C **3** 12394-12398.
- [16]. Qamar A, Phan H P, Han J, Tanner P, Dinh T, Wang L, Dimitrijević S, Dao D V 2015 Journal of Materials Chemistry C **3** 8804-8809.
- [17]. Qamar A, Phan H P, Dao D V, Tanner P 2015 IEEE Electron Device Letters **36** 708-710.
- [18]. Phan H P, Qamar A, Dao D V, Dinh T, Wang L, Han J, Tanner P, Dimitrijević S, Nguyen N-T 2015 RSC Advances **5** 56377-56381.
- [19]. Kanda Y and Yasukawa A 1982 Sens. Actuators **2** 283.
- [20]. Kanda Y and Yamamura K 1989 Sens. Actuators **18** 247.
- [21]. Kanda Y and Migitaka M 1976 Phys. Status Solidi A **38** K41.
- [22]. Ren T L, Tian H, Xie D and Yang Y 2012 Sensors **12** 6685-6694.